Proceedings of ASME Turbo Expo 2016: Turbine Technical Conference and Exposition
GT2016
June 13-17, 2016, Seoul, South Korea

GT2016-57485

COMPARISON OF FLAME TRANSFER FUNCTIONS ACQUIRED BY CHEMILUMINESCENCE AND DENSITY FLUCTUATION

Johannes Peterleithner, Riccardo Basso, Franz Heitmeir, Jakob Woisetschläger
Institute for Thermal Turbomachinery and Machine Dynamics, Graz University of Technology
8010 Graz, Austria

Raimund Schlüßler, Jürgen Czarske, Andreas Fischer
Chair of Measurement and Sensor System Techniques
Technische Universität Dresden
01062 Dresden, Germany

ABSTRACT

The goal of this study was to measure the Flame Transfer Function of a perfectly and a partially premixed turbulent flame by means of Laser Interferometric Vibrometry. For the first time, this technique is used to detect integral heat release fluctuations. The results were compared to classical OH-chemiluminescence measurements. Effects of equivalence ratio waves and vortex rollup were found within those flames and were then investigated by means of time resolved planar CH*/OH*-chemiluminescence and Frequency modulated Doppler global velocimetry. This work is motivated by the difficulties chemiluminescence encounters when faced with partially premixed flames including equivalence ratio waves and flame stretching. LIV, recording the time derivative of the density fluctuations as line-of-sight data, is not affected by these flame properties.*

NOMENCLATURE

c	[m/s]	speed of sound
D_{exit}	[mm]	burner exit diameter
f_D	[Hz]	Doppler shift of laser light
FTF	[-]	flame transfer function
G	[m³/kg]	Gladstone-Dale constant
$\vec{i}$	[-]	Laser incidence direction
I_{OH*} I_{CH*}	[-]	light intensity of OH* and CH*
k_{vib}	[mm/s/V]	vibrometer calibration constant
LIV		laser interferometric vibrometry
LDA		laser Doppler interferometry
i-OH*-CL		integral OH* Chemiluminescence
$\vec{o}$	[-]	observation direction
PPM		perfectly premixed
Q',	[W]	fluctuation of heat release
q_v'	[W/m³]	fluctuation of heat release
$\vec{s}$	[-]	sensitivity vector
TPM		technically premixed
u'	[m/s]	fluctuation of Axial velocity
U	[V]	voltage
$\vec{v}$	[m/s]	velocity vector
x, y, z	[mm]	coordinates
Φ	[-]	equivalence ratio
α	[°]	phase angle
ζ	[m]	length of measurement volume
K	[-]	ratio of specific heats
λ	[nm]	laser wave length
ρ	[kg/mm³]	density

INTRODUCTION

Modern gas turbines for power generation rely on premixed combustion systems to achieve high combustion efficiency and low emissions. As a drawback, high power densities and reduced damping capabilities of the combustor increase the susceptibility to thermoacoustic oscillations. These instabilities arise from the positive coupling between the fluctuations of pressure and heat release [1]. Prediction of gas turbine stability is often achieved by network models, originally used in system dynamics analysis. Within the model the flame remains a 'black box'. The flame is described as a single input single output block. Usually the data for this block comes from

Copyright © 2016 by ASME

flame transfer functions, which relate the unsteady heat release of the flame to perturbations of acoustic velocity at the burner exit [2, 3]. In the past, a variety of methods for the measurement of flame transfer functions in research combustors have been published. A method widely used for determining the FTF is measuring the chemiluminescence from OH* within the flame as the measure for heat release. Velocity fluctuations at the burner exit are obtained either directly from hot wire anemometry or laser Doppler anemometry. Whereas approaches relying on chemiluminescence are only applicable for adiabatic flames with low strain rates and constant equivalence ratio [4, 5], this method is not applicable to technically premixed combustion systems.

As an alternative Interferometric techniques like laser interferometric vibrometry (LIV) are not affected by this. They can detect heat release without the restriction of perfect mixing [6, 7]. The advantage of this technique is that it measures the time derivative of density fluctuations directly. With the absence of pressure fluctuations, this is a measure of heat release rate [8]. The link between those quantities has been exploited before, but this is the first time, integral heat release is recorded. As a benefit, it overcomes the time consuming process of traversing the whole field. In this study the technique is applied to a swirl stabilized burner configuration with a known flow field and well defined operating conditions. The flow is excited using a siren in the main air supply, where the perturbation level is measured with laser Doppler anemometry (LDA) in the burner exit nozzle. Secondly, integral Heat release is discussed for excitation frequencies from 0 Hz to 600 Hz. As a result from both, the flame transfer function can be calculated. This was done for a perfectly premixed flame, where chemiluminescence should provide a reliable result due to the absence of equivalence ratio waves. Then a technically premixed configuration more relevant to industrial applications is investigated. Differences in heat release are further analyzed by means of planar time resolved equivalence ratio measurements. To interpret the natural heat release spectrum of the flame, a Doppler global velocimeter with laser frequency modulation (FM-DGV) was used to compare the time resolved velocity field with line-of-sight-integrated heat release rate.

EXPERIMENTAL SETUP

For the investigations presented in this paper, a variable geometry burner was used and the flow was excited with a siren, mounted into the axial air-feedline. The burner has been documented in detail in the work of Giuliani et al [9], the flow-field and characteristics have been published recently [10] and the siren has been characterized in [11]. In Fig. 1 the burner is shown with the standard configuration - technically premixed (TPM) - to the left and the reference configuration - perfectly premixed (PPM) - to the right of the setup.

In the TPM configuration, the combustor is fed by fuel (a) tangential air (b) and axial air (c). The axial air is forced through a stratifier in order to ensure purely axial flow. In

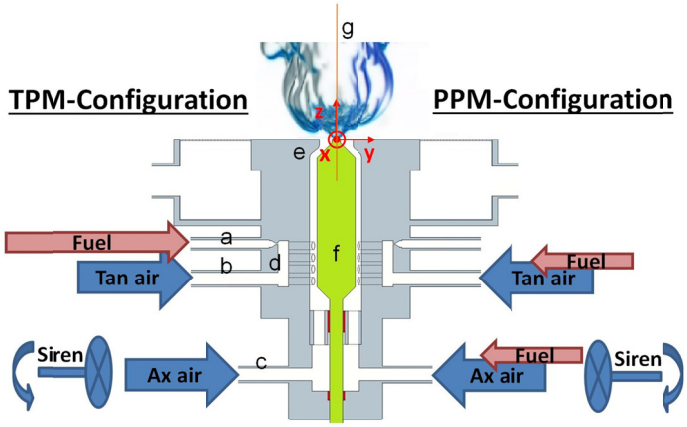

FIGURE 1: THE EXPERIMENTAL SETUP WITH THE TPM CONFIGURATION TO THE LEFT AND THE PPM CONFIGURATION TO THE RIGHT

contrast to this the tangential air passes the outer mixing chamber (d) and from there, enters the plenum through 32 cylindrical bores aligned tangentially and symmetrically around the burner axis. Methane is injected into the tangential air in the outer chamber. The siren modulates the axial air flow only.

In case of perfect mixing (PPM), the methane was injected into the air supply far upstream before tangential and axial air split. As shown in Fig. 1, the fuel is injected through small bores of a diameter of 0.5 mm. At those injectors a large pressure drop is present. Therefore, they are assumed to be acoustically stiff and the acoustics of the plenum would only slightly alter the fuel flow. Then equivalence ratio waves are enabled without necessarily generating large amplitudes of heat release.

TABLE 1: FLOW PROPERTIES

Axial air [g/s]	Tangential air [g/s]	Fuel [g/s]	Swirl Number [-]
0.422	0.397	0.0683	0.54

The movable center cone (f) of the burner was set to 1 mm above the exit in order to constrict the flow through the burner exit nozzle (e) and consequently ensure correct momentum for the point of operation. The test rig was set up in a thermoacoustic laboratory within a 3x3x2.5 m3 box with two layers of low reflective curtains and a sound absorbing ceiling. The mass flow, which was the same for both points of operation, can be found in Table 1. The simplified Swirl number, according to [2] neglecting the pressure term, was measured using a burner exit radius of 8 mm averaging over a height of z = 8.5 mm to z = 17 mm which is 0.5 times and 1 time the burner exit diameter respectively. The coordinate system for all measurements originates at the burner exit and the measurement plane (g) is defined by the x and z-axis.

Copyright © 2016 by ASME

Measuring Techniques

Heat release fluctuations for the FTF were acquired by means of LIV and OH*-chemiluminescense using a photomultiplier with a filter. Velocity fluctuations for the FTF were acquired by means of laser Doppler anemometry. For planar time resolved velocity fields, FM-DGV was employed, and finally the phase averaged planar CH*/OH*-chemiluminescence measurements were used to visualize equivalence ratio waves. Below the different measurement techniques are explained in detail.

Laser interferometric vibrometry (LIV) detects the line of sight (ζ) integrated density fluctuations of gasses by means of interferometry. This is shown in detail in [12] and applied in [13, 14]. Using a Polytec laser vibrometer (interferometer head OFV-353, velocity decoder OFV-3001, calibration factor 5mm/s/V, 200kHz bandwidth, no filters, Polytec, Waldbronn, Germany), the measured voltage (U) is linked to the derivative of the density fluctuation (ρ**)** by the Gladstone-Dale constant (G) which is 2.59e-4 m³/kg for the present points of operation and the calibration factor (k) which was set to 5 mm/s:

$$\int \frac{d}{dt}\rho(t)\, d\zeta = \frac{2 * k_{vib}}{G} U(t) \tag{1}$$

The link between density fluctuations and heat release fluctuations has been derived and extensively discussed by **[8, 6, 7]**. Neglecting pressure fluctuations which - for unconfined flames - are low compared to volumetric heat release rate q_v, the following equation applies:

$$\frac{d\rho}{dt} = -\frac{\kappa - 1}{c^2}\frac{dq_V}{dt} \tag{2}$$

With the ratio of specific heats (κ) and the speed of sound (c). In combustion application LIV is used to locally or globally detect heat release fluctuations. In order to locally resolve the heat release fluctuations, the vibrometer must be traversed in a two dimensional field **[14]**. Since for FTFs, only the space integrated information of the flame is relevant, the laser beam of the vibrometer was expanded to and collimated at a diameter of 81 mm and centered at a height of 40 mm above the burner exit plane in order to acquire the entire combustion fluctuations at once. For the comparison with vorticity, the vibrometers beam was narrowed down to 5 mm in diameter and traversed in two directions with increments of 5mm. The result was interpolated in order to provide more readable plots. Areas of uncertainty of the LIV technique include the varying Gladstone-Dale constant discussed in **[6]**, dependency on temperature discussed in **[12]** and a varying intensity of the laser beam over the beam diameter due to a Gaussian distribution of the laser light. Since only the central part of the beam covered the test section, the accuracy of the LIV detector signal is less than +/- 4 %, this can be further reduced, using a sufficiently strong light source.

Alternatively, for the FTF, the integral **OH*-chemiluminescence** (i-OH*-CL) intensity emitted by the flame was acquired using an UV filtered photomultiplier (PMM01, Thorlabs Inc., Newton, New Jersey, USA). On the photomultiplier a narrow band OH* interference filter (310 nm CWL, FWHM 10±2 nm Bandwidth, 50mm Mounted Diameter, 18 % Transmission, Edmund Optics, Barrington, NJ, USA) was mounted.

The processing of LIV and the i-OH*-CL signal were acquired with 100 kilosamples per second using a data acquisition with analog input modules NI-91215 (National Instruments, Austin, Texas) and Labview 8.6 software. The spectral analysis was performed using a fast fourier transform (FFT) based on Matlab routines. In order to tackle the scalloping loss of Fourier transforms, a Matlab 2015a implementation of a Flattop filter was used, which is valid if frequencies are known in advance, ensuring a high signal to noise ratio.

To record the velocities for the FTF a classical **laser Doppler anemometer** (LDA) was used to measure the axial velocity at the burner exit at z=2 mm x=r= 5.5 mm. (FibreFlow, DANTEC Dynamics, Roskilde, Denmark). Since LDA does not provide frequency spectra per se, with the help of a siren trigger the result was phase averaged and then divided into 64 bins. A FFT was performed on the phase averaged result and the base-frequency was used for the FTF.

A **particle image velocimetry** (PIV) was used as reference. The PIV setup was the same as in **[10]** with 1200 averaged images and two cameras set up at an angle of 45°.

A **Doppler global velocimetry** measurement system with laser frequency modulation (FM-DGV) was employed to assess the flame dynamics of the non-excited flame in part two of this article. The FM-DGV technique relies on measuring the Doppler frequency shift f_D of laser light, which is scattered by seeding particles moving with the flow:

$$f_D = \vec{v}\,\frac{|\vec{o} - \vec{\imath}|}{\lambda} * \frac{(\vec{o} - \vec{\imath})}{|\vec{o} - \vec{\imath}|} \;\; with \;\; \frac{(\vec{o} - \vec{\imath})}{|\vec{o} - \vec{\imath}|} = \vec{s} \tag{3}$$

with λ as laser wavelength, $\vec{o}$ as observation direction and $\vec{\imath}$ as laser incidence direction. Hence, the velocity component $v_{oi} = \vec{v} * \vec{s}$ along the direction of the sensitivity vector $\vec{s}$ (i.e., along the bisecting line of $\vec{o}$ and $-\vec{\imath}$) can be derived from the measured Doppler frequency. For determining the Doppler frequency shift, a frequency stabilized laser source in combination with a molecular cesium absorption cell with frequency dependent transmission was used. The frequency

Copyright © 2016 by ASME

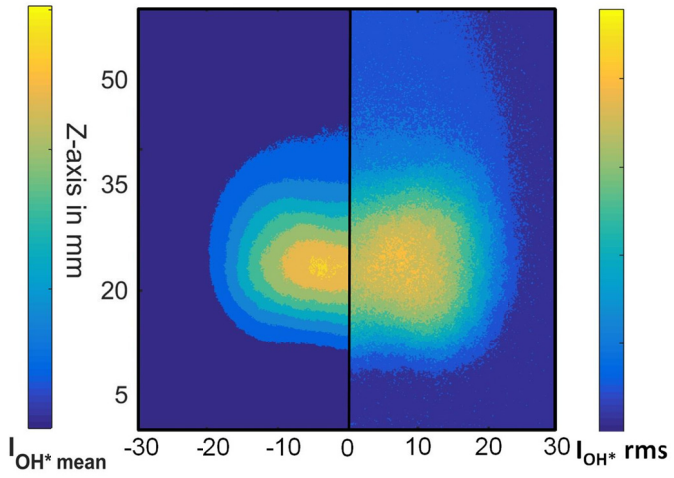

FIGURE 2: OH*-CHEMILUMINESCENCE OF THE TPM FLAME. MEAN (LEFT) AND RMS OF FLUCTUATION (RIGHT)

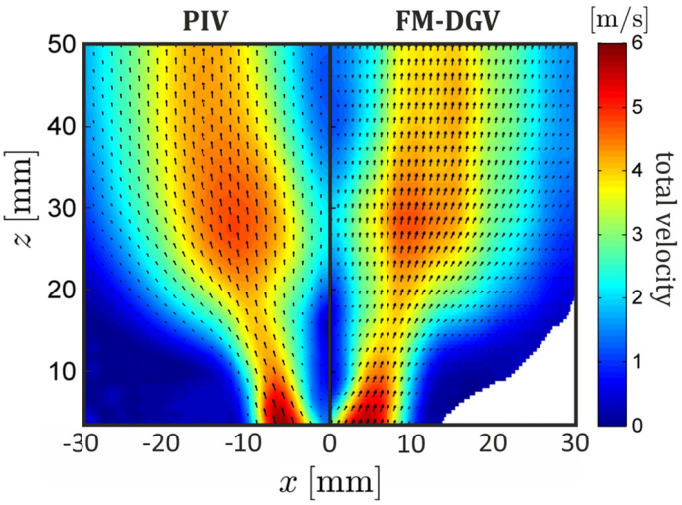

FIGURE 3: PIV (LEFT) AND FM-DGV (RIGHT) RESULTS OF THE MEAN VELOCITY FIELD.

shift can then be evaluated by measuring the intensity variation of the scattered light behind the absorption cell [15].

The applied FM-DGV system was described in more detail in [16]. It features a high-power continuous laser illumination with a maximum output power of 1 W at 895 nm (Toptica Photonics AG) for achieving a high signal-to-noise ratio. Also three observation directions were used, enabling simultaneous, three component measurements with a spatial resolution of 1 mm and a maximum measurement rate of 100 kHz. Hence, velocity spectra with up to a maximum frequency of 50 kHz can be resolved. A temporal averaging was applied for reducing the measurement uncertainty, resulting in a cut-off frequency for the velocity spectra of 2 kHz, which is sufficiently high to resolve expected flow structures.

The OH* and CH* acquisition providing the equivalence ratio waves were measured with a light-intensified camera (NanoStar, 1280x1024 Pixel, photocathode radiant sensitivity 310 nm/430 nm = 65 %, DaVis 7.6 Software, LaVision, Göttingen, Germany) and a OH* (above) or a CH* interference filter (430±2 nm CWL, FWHM 10±2 nm Bandwidth, 50 mm Mounted Diameter, 98 % Transmission, Edmund Optics, Barrington, NJ, USA). The camera was triggered by the siren with the images recorded phase resolved and then phase averaged. For phase steps α of 45° one hundred images were averaged according to:

$$\frac{\phi'(\alpha)_{xz}}{\bar{\phi}^{\ \alpha xz}} = \frac{\frac{I_{CH*}(\alpha)_{xz}}{I_{OH*}(\alpha)_{xz}} - \overline{\left(\frac{I_{CH*xz}}{I_{OH*xz}}\right)}^{\alpha}}{\overline{\left(\frac{I_{CH*}}{I_{OH*}}\right)}^{\alpha xz}} \qquad (4)$$

RESULTS

Stationary Flame Properties and Flow Field

The mean flame behavior and flow field will be discussed below on the example of the TPM case. The distribution of reacting gasses measured by OH*-chemiluminescence (Fig. 2 left) shows the main reaction zone just after 2xDexit downstream of the burner exit extending to a maximum of 2.5Dexit. The typical V-shape flame indicates that the reaction takes place in the inner shear layer of the jet only, while the reaction is quenched in the outer shear layer by heat loss and strain.

In this flame the fluid flow of the reacting gasses is dominated by the axial component (Fig 3). From half the burner exit diameter (D_{exit}) after the burner exit nozzle, the velocity decreases slightly due to swirl induced jet opening, which is caused by the sudden area change at the burner exit. At around $2xD_{exit}$ or 30 mm downstream the fluid starts to accelerate driven by expansion of the hot gases in the reaction zone, and from $2.5xD_{exit}$ gradually decelerates due to mixing with the ambient gasses. The mean velocity field for reacting gasses was acquired by FM-DGV and stereo-PIV. As shown in (Fig. 3) the agreement between the two different measurement techniques, FM-DGV and stereo-PIV is very good. This confidence check shows the reliability of the novel FM-DGV which was used to record velocity spectra as discussed below.

Flame Dynamics

Premixed swirl stabilized combustion is a highly dynamic process. Fig. 2 (right) shows the RMS value of OH*-chemiluminescence fluctuations. Comparison with the mean value (left) shows that the highest amplitudes of fluctuation are around the position of mean heat release. Below the fluctuations are more extended than above the flame. Looking at the spatially integrated heat release recorded by the photomultiplier (Fig. 4), the spectra for both operating points (TPM and PPM) look quite different. Both flame spectra show the typical features of a turbulent process. They peak at frequencies below 200 Hz and gently decrease towards higher frequencies. This is expected due to the comparably low velocities within the flame of around 5m/s (Fig. 3). The PPM's

Copyright © 2016 by ASME

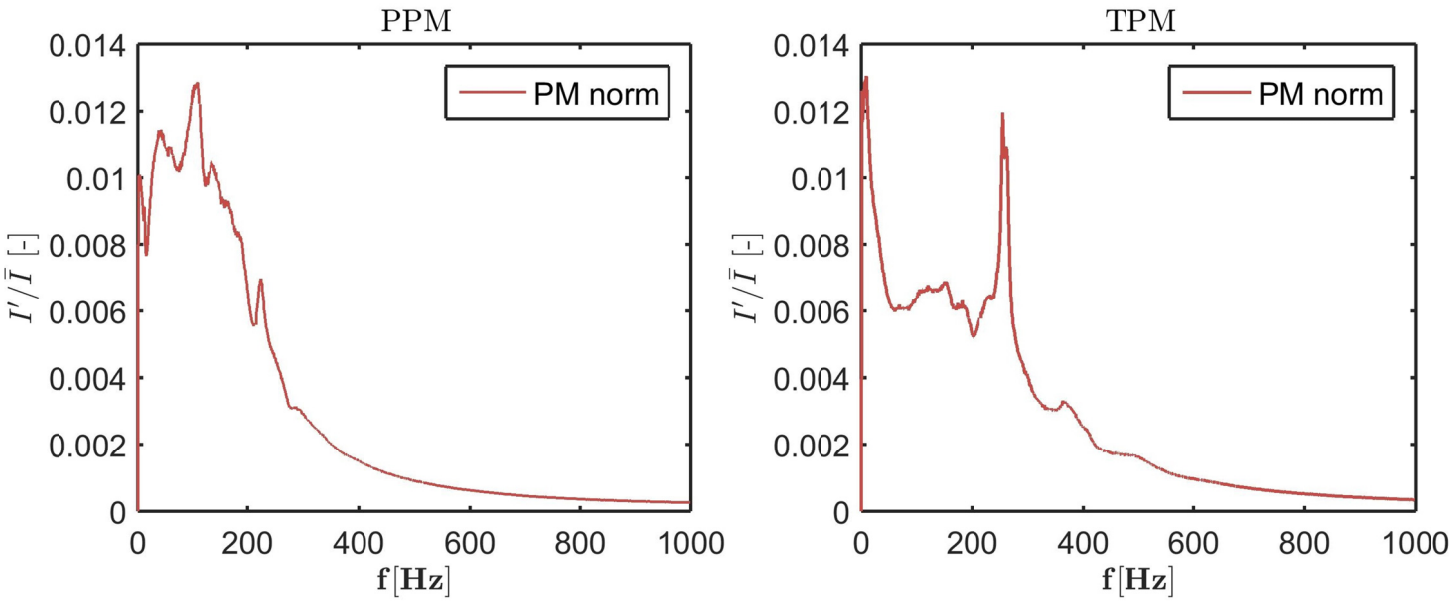

FIGURE 4: NATURAL SPECTRUM OF OH*-CHEMILUMINENCE FOR THE PPM (LEFT) AND TPM (RIGHT) TEST CASE.

broadband background peaks at around 125 Hz, which is considerably lower than the one of the TPM test case. Additionally the perfectly premixed flame shows a distinct peak at around 125 Hz, sitting on top of the smooth underground signal.

In contrast to this, the TPM case shows a lower overall fluctuation in the low frequencies. Secondly a very distinct peak at 250 Hz is recorded which is about twice as high as the broad band spectrum. This effect will be further discussed below.

Recording the Flame Transfer Function

In the folowing, the linear response of the flame to upstream excitation is investigated. By means of LIV and i-OH*-CL flame transfer functions (FTF) under TPM and PPM conditions are recorded. A comparison between both approaches is performed.

To investigate thermoacoustic stability of flames, recording the FTF is a common tool. FTF reduces the complex dynamic behavior of combustion to an amplitude and a phase plot. This information can be used for network models, where the flame is generally treated as a 'black box'. This model includes one input which is the fluctuation of velocity upstream of the flame, and one output which is the heat release fluctuation

$$\mathrm{FTF} = \frac{\dot{Q}'/\bar{\dot{Q}}}{u'/\bar{u}} \tag{5}$$

with the heat release fluctuation $\dot{Q}'$ mormalized by the mean heat release $\bar{\dot{Q}}$. This is then divided by the axial velocity fluctuation u', again normalized by its mean counterpart $\bar{u}$. There are several methods to acquire the FTF, most commonly from experiments. While [17, 18] have developed a purely acoustic method, called multi microphone method (MMM), still the most widely used approach is to measure the dynamic velocity just upstream of the flame and the heat release rate with i-OH*-CL.

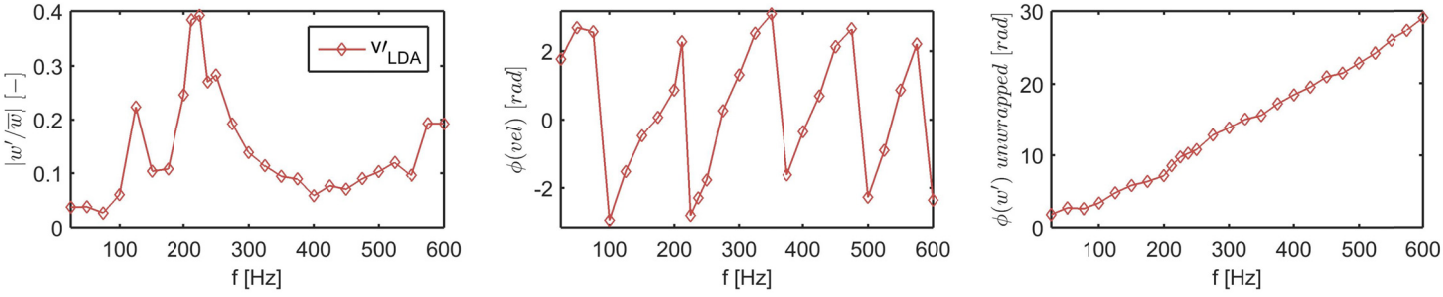

FIGURE 5: BURNER EXIT VELOCITY SPECTRA OF THE NON-REACTING FLOW.

Copyright © 2016 by ASME

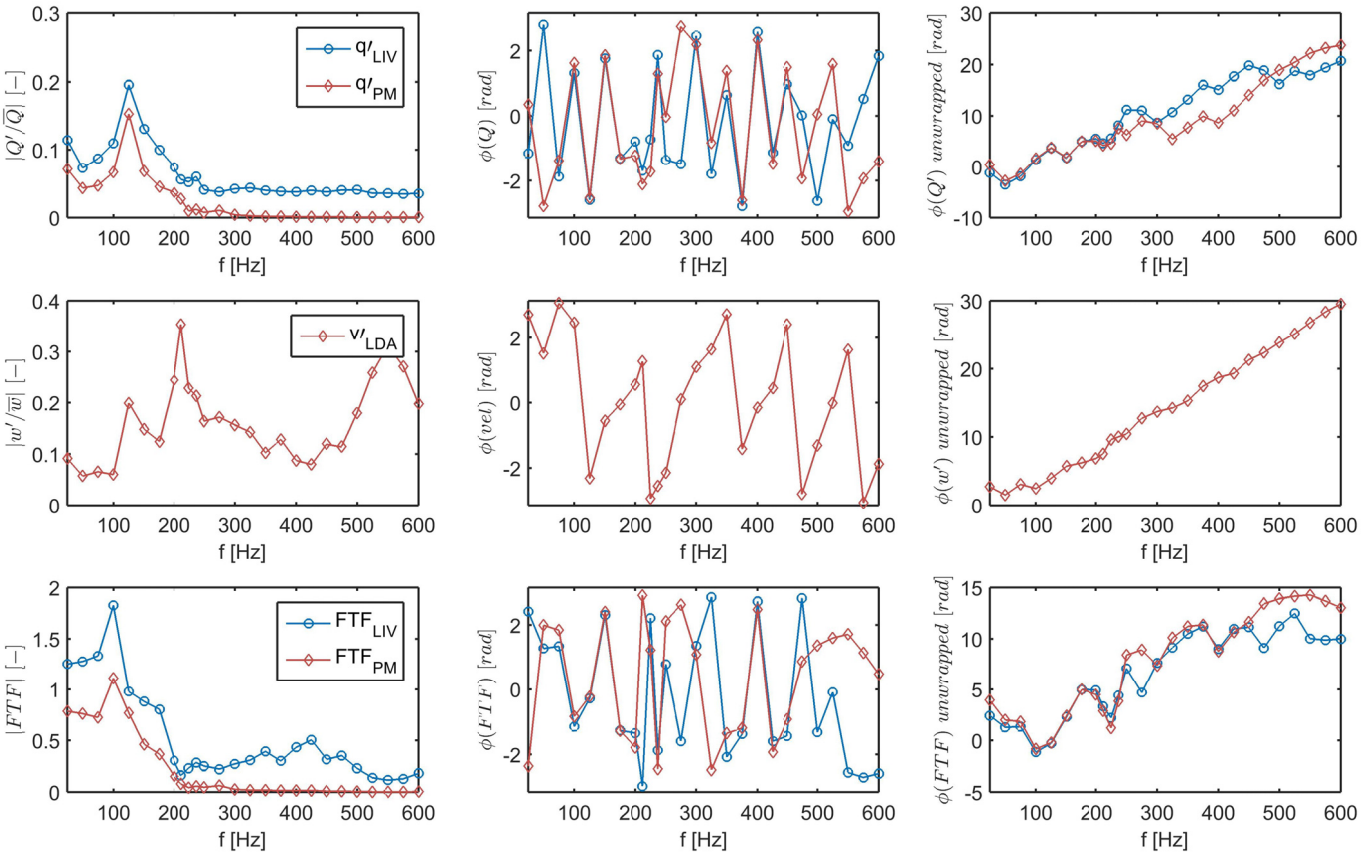

FIGURE 6: FLUCTUATIONS OF HEAT RELEASE, VELOCITY AND THE FTF FOR THE PPM TEST CASE WITH THEIR AMPLITUDE, PHASE AND UNWRAPPED PHASE RESPECTIVELY.

While it is a simple task to record the upstream velocity fluctuations causing the flame perturbations, unfortunately it is not so easy to acquire the heat release fluctuations quantitatively. I-OH*-CL is a commonly used optical measurement tool to assess the dynamics and heat distribution of flames. Mostly the OH*-radical emission is recorded by using an appropriate narrow band filter. Generally it is a comparably easy to use and low cost measurement technique. For perfect premixing where the equivalence ratio does not change with time, it is the most preferred tool for stability analysis. For a constant equivalence ratio the light intensity of the OH* radical is proportional to the heat release [19]. By normalizing the intensity by the mean value even the calibration factor can be avoided. The major drawback is its dependency on the equivalence ratio and the strain rate. This comes into play when partly premixed, so called 'technically premixed' flames are investigated. Then fluctuations of equivalence ratio can cause an overestimation of heat release fluctuations when measuring the OH*-chemiluminescence only [4]. Unfortunately most industrial combustion applications are not perfectly premixed, and therefore an alternative technique to measure heat release fluctuations is needed. LIV is a technique not significantly affected by equivalence ratio fluctuations.

LIV has proven to measure heat release in laminar flames and turbulent flames [6, 7, 20]. For technically premixed flames the technique is capable of recording the overall heat release fluctuations better than chemiluminescence techniques, since it is barely affected by equivalence ratio waves. Only a minor influence is present due to a change in the Gladstone-Dale constant. Following the above equations, the LIV measures the heat release not only qualitatively but also quantitatively. For the FTF the result was normalized by the mean power of the flame (3,4 kW) assuming a combustion efficiency of 100 %. The mean temperature of the flame was set to 1200 °C due to prior temperature measurements [21] and a cross-sectional flame area of 1000 mm^2 was used.

The **fluctuations of velocity** measured by LDA are shown in (Fig. 5) recorded without the reacting flame (flow only). The amplitude spectrum is plotted from 25 Hz up to 600 Hz. A strong overall modulation level of the bulk velocity of more than 5 percent of the mean flow proves that the siren modulation is strong enough to vary the velocity at the burner exit. Three significant peaks can be found in the spectrum, one minor peak at 125 Hz with about 20 percent fluctuation and one at 550Hz. The strongest fluctuation is however at 212 Hz with alsmost 40 percent fluctuation. The phase (Fig. 5 right) shows an increasing lag with increasing frequency.

Copyright © 2016 by ASME

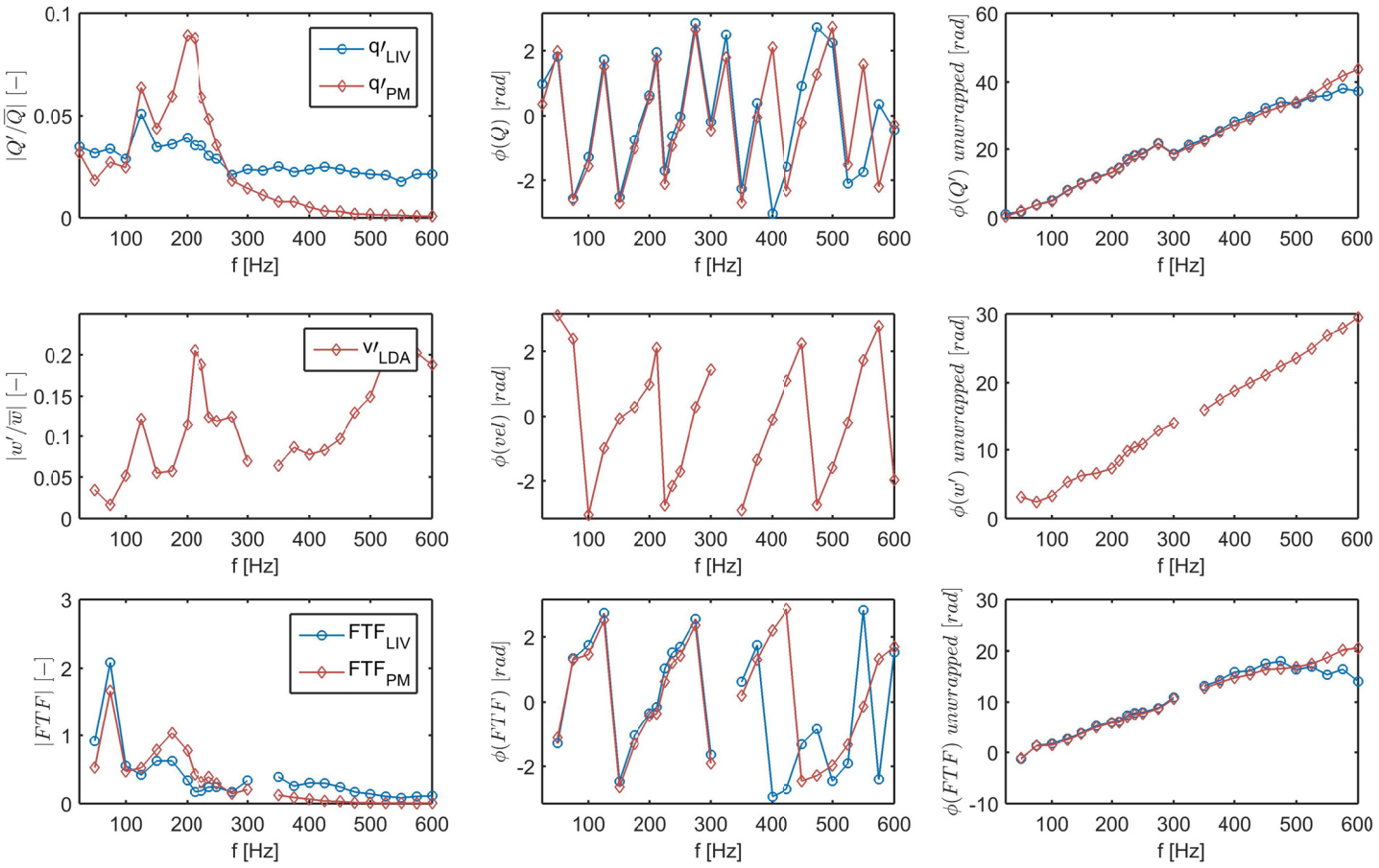

FIGURE 7: FLUCTUATIONS OF HEAT RELEASE, VELOCITY AND THE FTF FOR THE TPM TEST CASE WITH THEIR AMPLITUDE, PHASE AND UNWRAPPED PHASE RESPECTIVELY.

In Fig. 6 and Fig. 7 the relative heat release, the velocity and the FTF calculated from both, is shown for the test cases PPM and TPM. For both reacting cases, the velocity shows a similar trend as seen in the non-reacting flow (Fig. 5). This supports the expectation, that the flow field in the plenum upstream of the flame is not significantly changed by the different injection setups for TPM and PPM or the reaction itself.

Considering **heat release rate**, the typical behavior of flames acting as a low-pass filter is observed. Starting with PPM, the spectra of the photomultiplier and LIV match very well. The velocity-fluctuations discussed earlier, manifest themselves in the heat release causing a strong peak at 125 Hz. Other frequencies are widely suppressed, only minor fluctuations can be found due to the intense velocity fluctuation at 212 Hz. Over the whole spectrum, both measurement techniques match very well. The phase generally also matches over the whole frequency band.

When discussing the TPM test case (Fig. 7) a similar trend as for PPM can be found. Again at 125 Hz the flame clearly responds to the velocity fluctuations and again the 550 Hz peak is dampened due to the low-pass-filter characteristic of the flame but now the fluctuation at 212 Hz also affects the flame behavior. Although the LIV clearly detects increased fluctuations of heat release, it does not show a significant deflection compared to neighboring frequencies. In contrast to this, i-OH*-CL senses high amplitude at 212 Hz, which is more than 30 % higher than the fluctuation at 125 Hz. Thus, the assumption is that i-OH*-CL overestimates the heat release compared to the LIV. This strong overshoot in company of small heat release fluctuations can arise in configurations with large pressure drops over the injector. Then fluctuations of air flow hardly affect the fuel mass flow.

Although the amplitude values of i-OH*-CL and LIV do differ, the phase between both measurement systems matches very well. This means that the additional effect recorded by i-OH*-CL is roughly in phase with the heat fluctuations. Such an overestimation is expected for chemiluminescence measurements when equivalence ratio waves are present, which is possible in partially premixed flames and has been documented for example by [7].

Copyright © 2016 by ASME

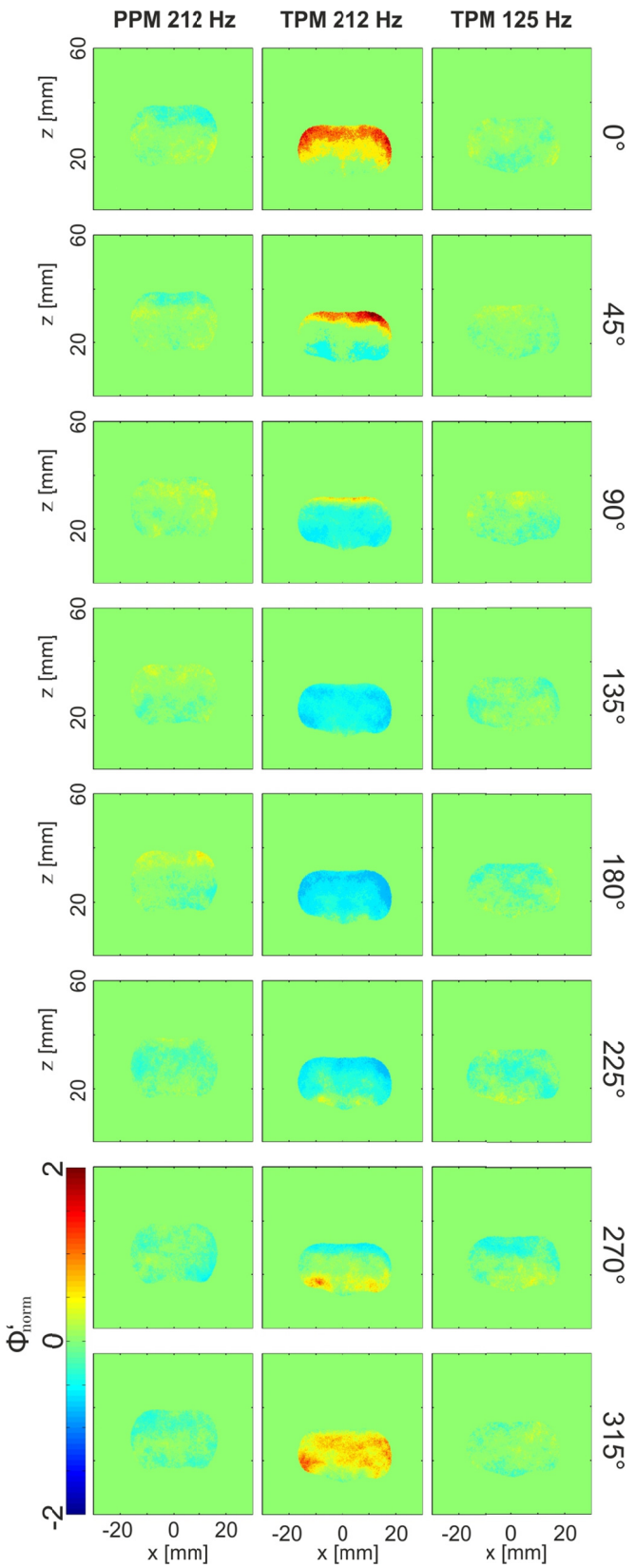

FIGURE 8: EQUIVALENCE RATIO WAVES AT DIFFERENT FREQUENCIES FOR BOTH TEST CASES.

The **flame transfer functions** of the PPM case shown in the last line of plots in Fig. 7 indicate similar trends for both measurement techniques. Since the same set of LDA velocity measurements was used for the FTF (i-OH*-CL and LIV), the difference is only caused by different recordings of heat release fluctuations. The stronger amplification at the LIV-FTF is because the LIV predicts a higher overall heat release fluctuation. Apparently, for both systems the major amplification is not at 125 Hz where both velocity and heat are high, but at around 100 Hz where heat fluctuation is high in spite of low velocity fluctuations. The phase for both measurement techniques matches well at regions where the amplitude is high and a good correlation is possible. The flame transfer function of the TPM case also shows the interesting result of high amplifications where velocity is low.

Equivalence Ratio Waves

Although heat release fluctuations are generally recorded correctly by both measurement techniques, a strong deviation in the heat release recordings by i-OH*-CL and LIV exists at 212 Hz for the TPM case. The hypothesis is that the chemiluminescence intensity recorded by the photomultiplier overestimates the heat release of the flame at 212 Hz due to an equivalence ratio wave being present. This assumption needs to be validated in order to correctly identify the influence of such an effect.

Chemiluminescence might not always represent heat release reliably, but it is a very good tool to measure changes in equivalence ratio [4]. Fig. 8 shows one cycle of equivalence ratio fluctuations ϕ' acquired by means of OH*/CH*-ratio measurements, following equation 4. For eight phase steps the normalized ϕ'-distribution across the flame is plotted. Regions of low signal-to-noise-ratio were masked. For the PPM test case at 212 Hz, the variations of ϕ are close to zero. Due to the mixing far upstream of the source of excitation for the PPM case, changes in equivalence ratio cannot appear. They are not exactly zero, because ambient air can mix with the swirled jet of reactants due to the unconfined flame setup. This however is a minor order effect compared to possible changes in equivalence ratio within the bulk flow. With regard to the uncertainty of such measurements it can be seen that wherever the signal is low (e.g. at the edges of the flame) measurement uncertainty increases. Therefore values in the center of the flame - where the signal-to-noise-ratio is high - are more reliable.

Considering TPM, the variations in ϕ are also close to zero for the 125 Hz case. This is expected, because there the agreement of both measurement techniques is good. However, at 212 Hz the TPM case exhibits violent oscillations in ϕ. This is exactly where the i-OH*-CL signal overshoots significantly compared to the LIV recordings. This measurement provides strong evidence that the OH*-Intensity overestimates the true heat release fluctuations of the flame.

Copyright © 2016 by ASME

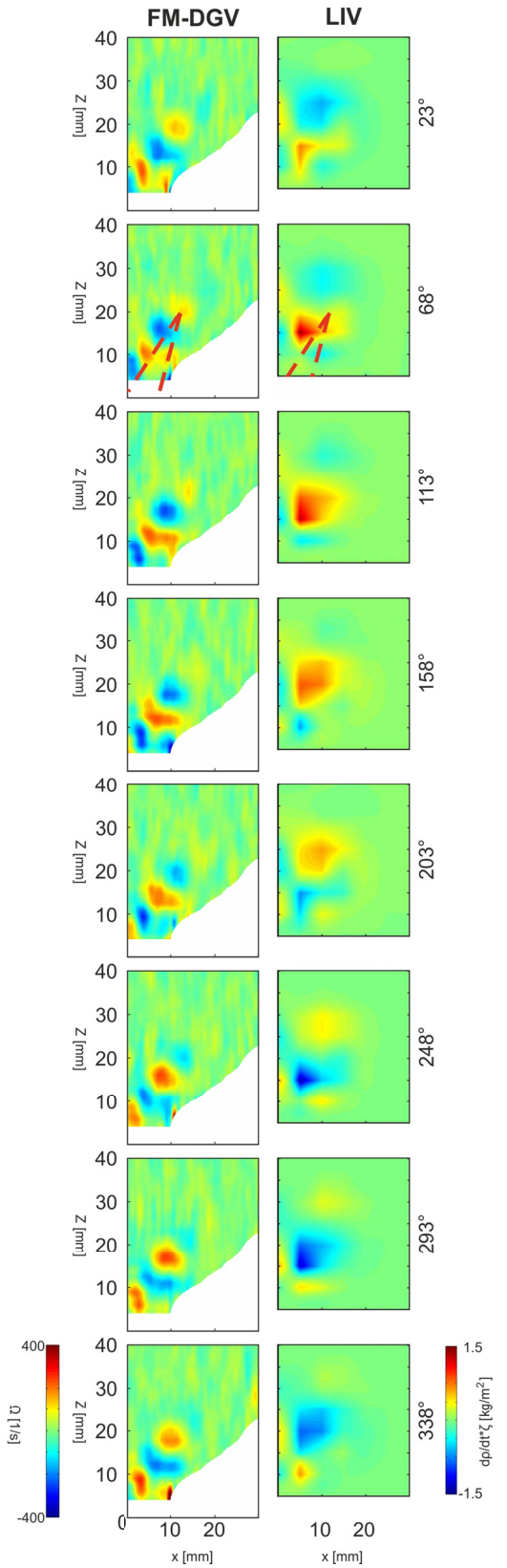

FIGURE 9: VORTICITY (LEFT, FM-DGV) AND HEAT RELEASE FLUCTUATIONS (RIGHT, LIV) FOR THE PULSATION AT 250HZ.

Comparison of Heat Release Fluctuations and Velocity Fluctuations

In the previous chapter, an overshoot of the i-OH*-CL signal in the FTF was shown at 212 Hz for linear excitation. It was identified as an equivalence ratio wave. This, however raises the question about the natural spectrum of i-OH*-CL at the TPM case where the most obvious effect can be found at 250 Hz. To identify the formation of this peak, the heat release is relevant, not only as integral data but also spatially resolved. In this chapter the heat release distribution (LIV) is investigated to trace the origin of this instability and compare it to vorticity fluctuations (FM-DGV) which are expected to interact with the flame front. The velocity signal from FM-DGV and the heat release signal from the LIV also identify the oscillation at around 250 Hz with several higher harmonics in the velocity spectrum.

For the dominant frequency of around 250 Hz a two dimensional cross-section of the flame was analyzed. A phase resolved evolution of heat and vorticity at this frequency is presented in Fig. 9. The photomultiplier signal served as phase-reference.

Comparing the **vorticity fluctuation** in Fig. 9 (left) with the mean flow and the mean heat distribution in Fig. 2 reveals that the vorticity is most dominant along the inner shear layer of the conical swirl-jet (illustrated in the second phase plot). It rises to a height of approximately 3 x D_{exit}. A second vortex can be found on the outer shear layer. It is less developed and starts in counterphase to the inner shear layer vortex. Both are caused by the velocity fluctuation coming from the plenum generating two counter rotating vortices, both veering off the center axis of the conical jet (right side of the flame). The swirl bends the jet and its shear layers outwards, away from the burner axis. Therefore the inner shear layer is longer than the outer one. As the undisturbed jet thins towards the tip of the cone, the vortices on both sides merge. However, quickly after detaching from the corner of the burner exit, the

outer vortex merges with the co-rotating one which detached 180° earlier. Looking at the time step 23° a positive vortex is about to detach from the outer corner of the burner (x = 10 mm, z = 5 mm) and a negative vortex is about to detach from the center body at (x = 0), but already at timestep 113° the outer vortex has reached the closest inner co-rotating one. By this the inner vortex street is amplified. Since it is the one which interacts with the flame, this could be the reason why exactly at this point of operation, the amplification is so strong. It seems that at this point of operation, velocity and swirl are just right to enable this merge of correlated swirls. Although the mean velocity remains high above the flame, no correlated vortices can be found.

The **heat release fluctuations** show pulsations in the same region as the mean heat release of the flame (Fig. 2). The strong pulsations are closer to the burner axis and just below the peak of mean heat release. While there is no pulsation below z = 10 mm (68° - 113°), the strongest amplitudes of heat release are reached at x = 5 mm and z = 15 mm, slowly decreasing towards higher levels. Due to lower measurement resolution less

Copyright © 2016 by ASME

obvious but still distinct, the fluctuations in heat release start at x = 5 mm, z = 10 mm and float down- and outwards following the inner shear layer of the right-side jet. For interpretation of the results, it is important to keep in mind that the measurement resolution is only 5 mm in comparison to 1 mm for velocity measurements.

Comparison of results from two measurement techniques shows that both fluctuations occur within the upper inner shear layer of the jet, which is also the lower part of the main heat release, and the region where the flame is anchored. Looking at the phase evolution, it shows that negative vorticity leads to positive heat release, which means that a vortex veering away from the jet curls up the surface of the flame. This leads to an increased surface area and consequently to an increased burn rate. At x = 5 mm and z = 15 mm the heat release is highest and this is also the region where the vortex fully hits the flame just after it merged and grew in strength. Here both measurement techniques acomplish each other, in order to gain insight into the flame dynamics.

CONCLUSION

The focus of this study was to discuss an alternative way of recording heat release rate and the FTF. It was the first time integral LIV was used for this application. The technique is promising of a better prediction of heat release in partially premixed (technically premixed) flames, where it is less receptive to equivalence ratio waves than the classical i-OH*-CL method.

Heat release spectra and FTF's for both perfectly premixed and technically premixed flames were analyzed. The trend of both systems correlated very well for the perfectly premixed flame as the literature suggests. While for the technically premixed case the agreement of the overall trends were good as well, a strong overshoot at one peak in the spectra of the i-OH*-CL signal was found. This was related to the known dependency of OH*-emission on equivalence ratio and correctly identified as such by visualizing the ratio between OH* and CH* fluctuations. A significant overshoot of OH*-CL without a considerable fluctuation of heat release can occur when the system features a high pressure drop over the injector. This acoustically stiff fuel line is then less sensitive to fluctuations of air flow. In the special case of this swirl-stabilized flame, the overshoot of the photomultiplier signal does not affect the FTF significantly because the trend of the FTF is mainly dominated by velocity fluctuations. Therefore the LIV method is an interesting alternative to i-OH*-CL in order to measure and quantify heat release fluctuations in perfectly as well as partially premixed flames. Secondly, naturally excited frequencies of the technically premixed flame were investigated, since the LIV technique clearly identified this effect as a heat release fluctuation. Time resolved velocity was an obvious quantity to investigate, in order to identify the root of these fluctuations. By means of FM-DGV the heat release fluctuation was tracked back to flame front roll up and consequently vorticity. Pulsations of heat release can be observed in the shear layer where the flame is anchored and where vortices hit the flame, heat release is in phase with the vortices. Detailed analysis of the plots identifies the vortices as the source of the heat release pulsations. This leads to the final conclusion that LIV is a promising technique for full field heat release measurements. It has been shown, that it is possible to measure the heat release rate of an unconfined flame. Similar to chemiluminescence, it is not free of restrictions. These include sensitivity of the Gladstone-Dale constant to mixture fluctuations, and sensitivity to temperature. Additionallly, care must be taken when adjusting the laser beam in order to maintain a homogenous illumination of the measurement volume.

ACKNOWLEDGEMENT

This research was partially funded by the Austrian Science Fund FWF within grant FWF-24096-N24 "Interferometric Detection of Thermoacoustic Oscillations in Flames". The authors would like to thank Prof. Thomas Sattelmayer, TU Munich for the fruitful discussions and all the support during this work.

References

[1] Rayleigh, "The explanation of certain acoustical phenomena," *Nature,* vol. 18, no. 455, pp. 319-321, 1878.

[2] S. Candel, D. Durox, T. Schuller, J. .. Bourgouin and J. P. Moeck, Dynamics of swirling flames, vol. 46, 2014, pp. 147-173.

[3] T. Sattelmayer and W. Polifke, "Assessment of methods for the computation of the linear stability of combustors," *Combustion Science and Technology,* vol. 175, no. 3, pp. 453-476, 2003.

[4] M. R. W. Lauer, Determination of the Heat Release Distribution in Turbulent Flames by Chemi-luminescence Imaging, Technische Universität München, 2011, pp. 147-173.

[5] B. Schuermans, F. Guethe, D. Pennell, D. Guyot and C. O. Paschereit, "Thermoacoustic modeling of a gas turbine using transfer functions measured under full engine pressure," *Journal of Engineering for Gas Turbines and Power,* vol. 132, no. 11, 2010.

[6] T. Leitgeb, T. Schuller, D. Durox, F. Giuliani, S. Köberl and J. Woisetschläger, "Interferometric determination of heat release rate in a pulsated flame," *Combustion and Flame,* vol. 160, no. 3, pp. 589-600, 2013.

[7] J. Peterleithner, N. V. Stadlmair, J. Woisetschläger and T. Sattelmayer, "Analysis of measured flame transfer functions with locally resolved density fluctuation and OH-Chemiluminescence Data," *Journal of Engineering for Gas Turbines and Power,* vol. 138, no. 3, 2016.

[8] A. P. Dowling and A. S. Morgans, "Feedback Control of Combustion Oscillations," *Annu. Rev. Fluid Mech.,* vol.

 Copyright © 2016 by ASME

37, pp. 151-182, 2005.

[9] F. Giuliani, J. W. Woisetschläger and T. Leitgeb, "Design and validation of a burner with variable geometry for extended combustion range," in *Proceedings of the ASME Turbo Expo*, 2012.

[10] J. Peterleithner, A. Marn and J. Woisetschläger, "Interferometric In estigation of the thermo-acoustics in a swirl stabilized Methane flame," in *Proceedings of the ASME Turbo Expo*, 2015.

[11] F. Giuliani, A. Lang, K. Johannes Gradl, P. Siebenhofer and J. Fritzer, "Air flow modulation for refined control of the combustion dynamics using a novel actuator," *Journal of Engineering for Gas Turbines and Power,* vol. 134, no. 2, 2012.

[12] J. Peterleithner and J. Woisetschläger, "Laser vibrometry for combustion diagnostics in thermoacoustic research," *Technisches Messen,* vol. 82, no. 11, pp. 549-555, 2015.

[13] N. Mayrhofer and J. Woisetschlaeger, "Frequency analysis of turbulent compressible flows by laser vibrometry," *Experiments in Fluids,* vol. 21, pp. 153-161, 2001.

[14] B. Hampel and J. Woisetschläger, "Frequency- and space-resolved measurement of local density fluctuations in air by laser vibrometry," *Measurement Science and Technology,* vol. 17, pp. 2835-2842, 2006.

[15] A. Fischer, J. König, J. Czarske, J. Peterleithner, J. Woisetschläger and T. Leitgeb, "Analysis of flow and density oscillations in a swirl-stabilized flame employing highly resolving optical measurement techniques," *Experiments in Fluids,* vol. 54, no. 12, 2013.

[16] R. Schlueßler, M. Bermuske, J. Czarske and A. Fischer, "Simultaneous three-component velocity measurements in a swirl-stabilized flame," *Experiments in Fluids,* vol. 56, no. 10, 2015.

[17] C. O. Paschereit, B. Schuermans, W. Polifke and O. Mattson, "Measurement of transfer matrices and source terms of premixed flames," *Journal of Engineering for Gas Turbines and Power,* vol. 124, no. 2, pp. 239-247, 2002.

[18] M. L. Munjal and A. G. Doige, "Theory of a two source-location method for direct experimental evaluation of the four-pole parameters of an aeroacoustic element," *Journal of Sound and Vibration,* vol. 141, no. 2, pp. 323-333, 1990.

[19] C. S. Panoutsos, Y. Hardalupas and A. M. K. P. Taylor, "Numerical evaluation of equivalence ratio measurement using OH* and CH* chemiluminescence in premixed and non-premixed methane-air flames," *Combustion and Flame,* vol. 156, no. 2, pp. 273-291, 2009.

[20] J. Li, D. Durox, F. Richecoeur and T. Schuller, "Analysis of chemiluminescence, density and heat release rate fluctuations in acoustically perturbed laminar premixed flames," *Combustion and Flame,* vol. 162, no. 10, pp. 3934-3945, 2015.

[21] T. Leitgeb, "On the Design and Validation of a Variable Geometry Burner Concept," Graz, 2012.

Copyright © 2016 by ASME